NASA Technical Memorandum 101648

Analysis and Test of a 16-Foot Radial Rib Reflector Developmental Model

Shawn A. Birchenough

August 1989

National Aeronautics and Space Administration

Langley Research Center
Hampton, Virginia 23665-5225

Analysis and Test of a 16-Foot Radial Rib Reflector Developmental Model

Abstract

Analytical and experimental modal tests have been performed to determine the vibrational characteristics of a 16-foot diameter radial rib reflector model. Single rib analyses and experimental tests provided preliminary information relating to the reflector. A finite element model predicted mode shapes and frequencies of the reflector. The analyses correlated well with the experimental tests, verifying the modeling method used. The results indicate that five related, characteristic mode shapes form a group. The frequencies of the modes are determined by the relative phase of the radial ribs.

Introduction

Many proposed spacecraft for earth observation consist of a platform-type truss structure which may support several payloads, including a large-diameter antenna. To reduce weight and possibly launch package volume, these will likely be light-weight and flexible. Flexible vibrations can degrade antenna pointing accuracy by making a target difficult to track with the antenna, for example. Therefore, vibration suppression systems are desirable. Active vibration suppression coupled with a real-time, closed-loop control system have the potential of damping a vibrating spacecraft.

Ground tests allow researchers to gain knowledge of the dynamics of a structure with a closed-loop, vibration-suppression system and to validate analyses and designs. The Controls Structures Interaction Office (CSIO) at the NASA Langley Research Center is currently planning closed-loop control ground tests on a platform-like structure consisting of a long truss and a large reflector. Since this test article is likely to be modified as the test program proceeds, it is referred to as the Evolutionary Model. Figure 1 shows the CSI Evolutionary Model configuration with the reflector in place. (The reflector analyzed and tested did not have a sensor plate attached. This sensor plate will be added in the future.) The purpose of this paper is to describe the designing, analytical modeling, and experimental testing of the reflector component of the test article. The reflector model is shown in Figure 2. Correlation between analytically predicted vibrational frequencies and experimental vibrational frequencies is presented. With this correlation and with the similarities between analytical and experimental mode shapes, the finite element modeling technique is validated.

Configuration Changes

The design of the reflector included determining its shape, size, and material. For the purposes of the CSI tests, three important design criteria were imposed on the reflector: a large diameter, small deformations under a gravitational load, and a low fundamental frequency. The primary constraint was that the reflector have small deformations due to gravity since it was to be ground tested. The reflector configuration had to be changed several times before the design criteria were met.

The original reflector configuration was quite flexible. It used very thin, hinged-free ribs and two sets of shaping cables. The eight long, thin, aluminum radial ribs (8 ft. x 2 in. x 1/16 in.) were hinged at the hub (a round aluminum plate) and were spaced at 45-degree increments. The length and thickness of the ribs were sized for a rib natural frequency of approximately 2 Hz. One set of cables between the tips of the ribs caused the ribs to buckle into a dished shape. The second cable set provided tension and stability from behind each rib (connecting at the 3/4 length point on the rib), causing all of the ribs to buckle in the same direction. Each cable in this second set attached to a rod which passed through the hub. When erected, so that the face plane of the reflector was

perpendicular to the ground plane (the actual test position), the gravitational force on the ribs caused them to deform excessively.

An iteration on this original design called for thicker ribs with less weight. The geometry remained the same, but 1/4 in. thick, pultruded fiberglass ribs replaced the thin aluminum ones. All of the ribs did not have the same prestressed shape due to irregularities throughout the pultruded fiberglass material. Therefore, the material for the reflector ribs was changed back to aluminum.

A third reflector model used 1/4 in. thick aluminum ribs which were 2 in. wide. The two cable sets were used again, as in the preceding configuration. When placed in the test position, the center rod showed a large amount of deflection due to the length of that rod and the weight of the thick aluminum ribs it had to support. Another change in the reflector design was necessary.

The next reflector configuration changed the original design substantially. The center rod was removed as well as the set of cables connected to it. The ribs (aluminum, 1/4 in. thick and 1 in. wide) were bolted to the hub, instead of pinned. The tension in the cables connecting the tips of the ribs gave the reflector a slight dish shape. When erected in the test position, the ribs again sagged excessively. The deflections, however, were not due to the thickness, but were due to the rib width. The ribs extending from the sides of the reflector twisted near the tips because of a small moment of inertia about an axis running along the rib. This condition indicated that the ribs needed a larger width.

The final design uses an aluminum rib 1/4 in. thick and 2 in. wide, see Figure 3. The tension in the single set of cables at the rib tips shape the reflector. When erected into the test position, the ribs deflect a small amount. This final reflector meets two design criteria: small deflections in a gravitational field and a large diameter, approximately 16 ft. Additionally, this design has a small static torque compared with the other designs. Information on meeting the third criterion, the low vibrational frequency, was provided by the experimental tests and the finite element model analyses.

Reflector Description

As described above, the reflector configuration consists of 8 radial ribs, a set of cables and a central, round hub as shown in Figure 3. The finite element model of this configuration was generated. Also, this was the reflector tested in the laboratory. The 8 radial ribs measure 93.25 in. long, 0.25 in. thick, and 2 in. wide. Each of these ribs extend radially from the center of the hub, which is a 3/8 in. thick plate with an 8 in. radius. The ribs are oriented 45° apart around the hub. Each rib overlaps the hub by 5.25 in. and is bolted to the hub. Therefore, the distance from the rib end to the hub center is 2.75 in. The overlap gives the flat reflector a diameter of exactly 16 ft. from one rib tip to the opposite rib tip, before the cables are tightened. The bowl-shape of the reflector is caused by circumferential, tensioning cables which hold the ribs in a prestressed shape. The set of cables connecting the rib tips consists of 8 separate steel cables, 1/32 in. diameter. One end of a single cable attaches securely to one rib tip. The other end of this cable loops around a thumb screw on the tip of an adjacent rib. The thumb screw winds to adjust the length of the cable, and therefore the tension. This set-up continues around the reflector for each of the ribs. From the dimensions and configuration of the single rib model (refer to Single Reflector Rib - Configuration, below), the distance between the deformed rib tips was calculated using the geometric relationship in Equation 1.

$$l_c = 2r\cos B \qquad (1)$$

The distance between ribs (l_c = 71.75 in.) was set by adjusting the cable length. The radius of the reflector, r, is 93.75 in. (91 in., as in the single rib model, plus 2.75 in. of the hub that is not overlapped).

The angle, B = 67.5°, is defined between a rib and a cable connected to that rib. The prestressed structure has a diameter of 187.5 in. (15 ft. 7.5 in.) with a depth of 18 in., measured from the hub to the plane passing through the ribs tips.

Figure 3 indicates that each cable carries 9.44 lbs. of tensile force. This value comes from the geometric relationship in Equation 2, knowing the force on the cable in the single rib model (refer to Single Reflector Rib - Configuration).

$$Tr = Ts/2\cos B \qquad (2)$$

The cable tension in the reflector and in the single rib model are Tr and Ts respectively. The factor of $1/2$ is necessary because the tension from 2 cables acts on each rib in the reflector. Table 1 lists the actual tension measurements taken on each of the 8 cables with a tensiometer. The numbers correspond to the cable numbers in Figure 3. The discrepancies between the calculated and the measured values result from differences in the gravitational load direction for each rib and from slight differences in the individual rib dimensions.

The reflector mounts via four large bolts through the hub, to the backstop in the laboratory of building 1293B as shown in Figure 2.

Before testing the reflector for its vibrational properties, it was necessary to perform preliminary analyses and tests.

Single Reflector Rib

A single rib was analyzed and tested to determine its natural frequencies. The results provided vibrational and static information applicable to the reflector model.

Configuration

As shown in Figure 4, the single rib model closely approximates a rib in the reflector. Physically, the long strip (2 in. x 0.257 in. x 93.25 in.) of 6061-T6 aluminum is bolted to an I-beam. This I-beam was secured to the floor of the laboratory. A hinge fastened to the free end of the rib provided a means for attaching a cable. The cable ran perpendicularly to the I-beam and had a thumb screw at that end to adjust the length of the cable. When the cable was tightened, the rib deflected into a bowed shape. For the test, the rib tip had a deflection of 18 in. while the cable carried a 7.23 lb. load. In this deformed shape, the tip of the rib was 91 in. from the I-beam. The rib length, measured from the securing bolts to the tip, is the same in this single rib configuration as in the reflector. The rib remained in this prestressed condition throughout the vibration tests and was modeled in the finite element model.

Analytical Model

A finite element model (FEM) provided accurate static and vibrational data to confirm tests performed in the laboratory. The Engineering Analysis Language (EAL)[1] FEM contained 9 elements: 1 for the cable and 8 for the aluminum rib. The standard property values for steel and aluminum were used for the cable and rib respectively. The rib elements were input as rectangular beams with the correct dimensions. A rod element was used to represent the cable.

The geometry and preloads needed to be modeled correctly in the FEM so that the final stiffness closely duplicates the stiffness of the test article. With the hardware, the force caused by the wire tension deforms the rib to give a bowed shape. Since EAL is only valid for linear systems with small deflections, these large deflections cannot be accurately modeled in the FEM by applying a cable load to the undeformed rib. Therefore, a method for both shaping the rib and preloading the members needed to be developed for the FEM.

The shape of the rib was formed from the coordinates of the node points. The coordinates of each node point in the FEM, without any preload in the elements, match those of points along the stressed,

single rib model in the laboratory. Therefore, the unstressed FEM has the same shape as the test article.

The compressive preloads in the rib elements were calculated by an independent section of the EAL input file. In this section, a force vector was temporarily applied at the rib tip. The load had a magnitude of 7.23 lbs. and pointed downward, along the cable. The magnitude and direction of this vector matched the cable load. No other preloads or forces were applied; this section was run solely to determine the loads in each of the rib elements. The results are tabulated in Table 2. The element numbers correspond to those in Figure 4. The results show that the elemental loads increase along the rib from the tip to the base.

After the elemental loads were determined, these loads were permanently applied as thermal loads. Knowing the forces on the elements (F), the following equation was used to calculate the appropriate temperature changes (ΔT) to be applied across those specific elements.

$$\Delta T = F/\alpha EA \qquad (3)$$

The coefficient of thermal expansion (α) and the elasticity modulus (E) were input with the material properties. Since the coefficient of thermal expansion is only used for the preloads, its actual value is not used in the EAL runstream. A calculated coefficient eases the numerical computation. The cross sectional area (A) was calculated from the elemental dimensions.

The change in temperature applied to preload the cable element was calculated using Equation 3. A negative coefficient of thermal expansion listed with the cable material properties indicated that this thermal load is tensile instead of compressive.

After defining the cable and rib preloads, they were applied in the EAL program. Since the deformed geometry was input, the preloads along the rib were input separately on the rib elements. The thermal change across the cable induced a preload which matched that in the laboratory set-up, 7.23 lbs.

The output from the first run indicated that two problems existed with the modeling method. First, the correct thermal loads were not induced across either the cable element or the rib elements because the elements were free to move. The elements needed clamped-clamped ends for the full thermal effect. Second, the ribs deflected from the zero-load shape. Since the nodal coordinates already matched the desired bowed shape, any additional deflection caused an incorrect final rib shape. Both of these problems were solved by applying a second constraint case.

A second constraint case was applied to the structure to embed the preloads in the stiffness matrix before performing a vibrational analysis. By constraining all the degrees of freedom at every node point, the rib did not deflect and the thermal changes induced the correct loads. The KG-matrix, a differential stiffness matrix associated with the fully constrained and internally loaded structure, is created after preloading the structure. Then, the KG-matrix is added to a general stiffness matrix (K-matrix). This K-matrix is initially created with the material properties, nodal geometry, and elemental dimensions. The sum of the K-matrix and the KG-matrix forms a new K-matrix. With the appropriate stiffness due to the embedded preloads, the fully constrained condition was removed. Then a vibrational analysis was performed on the structure with the correct constraint case. The first 4 frequencies and the associated mode shapes are shown in Figure 5.

Testing and Results

Vibrational tests were performed on the single reflector rib to confirm the analytical results. A hammer was used to excite the structure, and an accelerometer at the tip of the rib measured the excitations. A two-channel Hewlett-Packard 3562A Dynamic Signal Analyzer conditioned the data generated by the load cell in the hammer and by the

accelerometer. A force window placed on the excitation channel allowed the first part of the time record to pass while completely attenuating the last part. This type of window is effective with impulse excitations because the signal for the initial impact is recorded while residual effects are attenuated. An exponential window on the response channel attenuates the signal at an exponentially decaying rate determined by an input time constant. Also, this analyzer calculated an averaged frequency response function (FRF) after twenty separate FRF's were generated. The averaged FRF is shown in Figure 6 with the phase plot shown below. The sharp peaks and the 180° phase shifts at these peaks mark the natural frequencies of this structure. For comparison with the analytical frequencies, the first 4 experimental frequencies are given in Figure 5. With only one accelerometer, experimental mode shape data is not available.

Discussion

A high degree of correlation exists between the predicted and measured frequencies. The discrepancy in the 2nd mode frequencies results from the clamped condition at the base of the rib. The FEM perfectly models the clamp. The test article can not be perfectly clamped in the laboratory.

This high degree of correlation gave confidence that the discretization of the rib was sufficient for use in the reflector FEM. The next step included analytically modeling and testing the reflector. See the Test Results and Discussion section for correlation between the single rib results and the reflector results.

Reflector Analytical Model

A descriptive and accurate analytical model is essential to predict the vibrational effects of the actual structure. The FEM contains analytical approximations of each of the components which comprise the reflector. Also, preloads are placed in the FEM cables and ribs. The Appendix contains the EAL runstream for the reflector FEM.

Common beam elements and material properties describe the reflector model. Nine beam elements (10 nodes) comprise each rib, the ninth element overlaps and connects to the hub. The elements have the properties of aluminum and measure 1/4 in. thick and 2 in. wide. Sixteen plate elements (8 triangles and 8 trapezoids) fit together to form the hub. These elements have a 3/8 in. thickness. The octagonally shaped hub of the FEM weighs less than the actual circular hub. Lumped masses placed at the rim of the octagonal hub replace this weight difference. Rod elements, 1/32 in. diameter, with material properties of steel wire describe the cables. The bolts connecting the ribs to the hub and the hub to ground are represented by 1/4 in. diameter steel, tubular elements. Five degrees of freedom, 3 translational and 2 rotational, were constrained to zero on the four bolts representing connections to ground. The third rotational degree of freedom, about the bolt axis, was left free. All of the other nodes had six degrees of freedom free.

The approach used for applying the preloads in the single rib model was now used for the reflector model. Refer to the Single Reflector Rib - Analytical Model.

Unlike the single rib model, the reflector dynamics were affected by gravity. Therefore, the new K-matrix had another addition when a gravitational load was applied to the structure. The gravitational load simulates the force the structure is subject to while secured to the backstop as shown in Figure 2. Vectors point the gravitational load in the same direction with respect to the structure as the gravitational vector in the laboratory. Because the gravitational force affects the stiffness of the structure, it is added to the new K-matrix through a second KG-matrix. The sum of the new K-matrix and the second KG-matrix gives a final K-matrix which is used in the vibrational analysis. Both the thermal preloads and

the gravitational load are embedded in the final structural stiffness. Also, the vibrational analysis is performed on a structure with the correct constraint case.

Analytical Results

Table 3 lists the first 11 natural frequencies while Figure 7 shows the mode shapes. Mode 1 of Figure 7 indicates the rib numbering scheme which will be used in describing the mode shapes.

Mode 1 exhibits a rocking motion about the hub of the reflector involving some bending of the ribs. Mode 2 is referred to as the "butterfly" or "saddle" mode. In this mode, two sets of 2 ribs, namely ribs 2 and 6 and ribs 4 and 8, vibrate 180° out-of-phase with respect to each other. In mode 3, two sets of 3 ribs vibrate completely out-of-phase, namely ribs 3, 6, and 8 and ribs 2, 4, and 7. Two sets of 4 ribs vibrate out-of-phase in the 4th mode. This symmetric mode shape involves ribs 2, 4, 6, and 8 in one set; the remaining ribs form the second set. All the ribs move in-phase in the 5th mode. Each rib in the first 5 modes deforms like the first bending mode of the single rib model. Different coupling combinations of this one rib shape characterize the five separate reflector mode shapes. See the Test Results and Discussion section for further discussion on the mode shapes and frequencies.

Due to the cyclic symmetry of the structure, the first 3 modes have a pair of eigenvalues. These pairs result from the two planes of symmetry in the structure, set apart by a 45° angle. One mode shape of each pair differs from the other by a 45° rotation of the structure.

Experimental test results confirmed the method used to analytically model this reflector.

Instrumentation and Test Procedure

The vibrational testing was performed to validate the analytical modeling method. The reflector hung from the backstop in the laboratory. A standard hammer test was performed. The transducers used were a PCB impact hammer with a load cell and three PCB Structcel accelerometers. A soft tip on the hammer helped excite the low frequencies of the reflector. A GenRad 2515 Computer-Aided Test System processed all of the data from the transducers.

Since the rib tips deflected the most, all of the transducers were placed there. The impact hammer struck a single rib tip in a single direction throughout all of the testing. This kept the excitation point constant. Eight response points (1 at each rib tip) were necessary to describe the first 5 mode shapes. Therefore, the three accelerometers were moved after recording data at a response point. Three frequency response functions were recorded and averaged together at each of the 8 test locations. The structure was allowed to freely decay as the measurements were recorded. After conditioning and storing all of the necessary data, the GenRad used a polyreference curve fitting program to fit the final frequency response functions. From those curve fit functions, the natural frequencies, damping values, and the relative amplitudes were calculated. These parameters defined the experimental mode shapes, which were animated on the GenRad.

Test Results and Discussion

The calculated data gave information on the response of the experimental model of the reflector. Though not shown in this paper, the mode shapes generated by the GenRad system duplicate the shapes calculated by the EAL program. Table 3 compares the analytical and experimental frequencies. The experimental results compared well with the analytical results.

Mode Shapes

The vibrational characteristics of the reflector were described by mode shapes from both the FEM and the experimental model. Also, the single rib mode shapes provided information relating to the reflector. The mode shapes of the reflector can be classified into specific groups. A group is defined as a series of mode shapes, each of which has a single, characteristic bending shape for any individual rib. For example, the first five bending modes belong to the same group because all of the individual ribs, in each mode, have the same local shape. Table 3 lists the frequencies of the mode shapes in the first two groups. For the first group, the local rib mode shape corresponds to the first bending mode shape of the single rib model. Each rib in the modes of the second group has a shape which corresponds to the second bending mode shape of the single rib model, and so on. Different relative positions of these individual ribs define the global mode shapes of the reflector.

Within each group, there are 5 distinct global mode shapes, see Table 3. These modes are sequentially labeled with mode numbers (m = 1, 2, 3, 4, 0), where m is the number of complete sinusoidal cycles formed around the circumference of the reflector at the cables. To visualize the sinusoid produced by the cables, the 3-axis displacement is plotted versus the rib number. The undeformed shape is the zero line for the 3-axis. Figure 8 illustrates the procedure for determining the mode number. The m = 2 mode for the first mode shape group is shown in Figure 8.

As described in the Analytical Results section, the first 3 mode shapes of each group are sets containing two similar mode shapes with similar frequencies. See Table 3. These double values result from the symmetry of the reflector. The only difference between the similar mode shapes is a 45° rotation. The m = 4 mode shape in each group does not have a double value because a rotation of 45° results in the exact same mode shape. Also, the m = 5 modes are unique and do not have double values.

Frequencies

Table 3 shows that the 5th and 10th bending frequencies (the frequencies of the m = 0 mode shapes in Groups 1 and 2) match closely with the 1st and 2nd single rib frequencies given in Figure 5. The correlation between the m = 0 global mode and the single rib frequencies is expected. The ribs in the m = 0 mode are all in phase and all deflecting to the maximum amount for the group. This m = 0 configuration creates the most energy and, hence, the highest frequency for any mode shape in the group.

However, the frequencies for the m = 1 to m = 4 global modes are lower than the frequency of the m = 0 mode. The frequencies of these modes are determined by the number of ribs vibrating out-of-phase. In the m = 4 mode, adjacent ribs are out-of-phase. This shape, with four ribs in phase and four ribs out-of-phase, contains a large amount of energy. Therefore, the m = 4 frequency is higher than the m = 3 frequency, which has only 3 ribs 180° out-of-phase with 3 other ribs. A similar explanation can be used for the m = 2 and the m = 1 frequencies.

In summary, the ribs vibrate to the maximum displacements in the m = 0 modes. This condition has the most energy for the entire group. From the m = 1 to m = 4 modes, the energy and frequencies increase in relation to the number of ribs vibrating out-of-phase.

Concluding Remarks

In this paper, the design, analysis, and vibrational test of a 16-foot radial rib reflector model have been described. The characteristic mode shapes and frequencies have been documented. The analytical predictions, based on the FEM, correlated well with test results for the first five reflector modes. The closely matched frequencies and similar mode shapes of the analysis and test confirmed the analytical modeling method.

The author would like to extend his thanks to Dr. Garnett Horner for his guidance and support through this project. Also, Harold Edighoffer, Jim Bailey, and Paul McGowan deserve thanks for their help.

Reference

[1] Whetstone, W. D., *EISI-EAL Engineering Language Reference Manual*, Engineering Information Systems, Inc., San Jose, 1983.

Table 1. Measured Cable Tension. Refer to Fig. 3

Cable number	Tension (lb.)
1	9.83
2	9.42
3	9.86
4	10.74
5	8.65
6	9.98
7	10.19
8	8.91

Table 2. Analytical rib element loads. Refer to Fig. 4

Rib Element	Prestress Force (lb.)
1	6.87
2	6.94
3	6.97
4	7.04
5	7.09
6	7.16
7	7.20
8	7.22

Table 3. Analytical and Experimental Frequencies with mode type and number

Mode (type)	Mode Number	Analytical Freq. (Hz.)	Experimental Freq. (Hz.)
1 (bending)	1	1.55	1.51
		1.55	
2 (bending)	2	1.63	1.64
		1.64	
3 (bending)	3	1.95	1.97
		1.98	
4 (bending)	4	2.13	2.13
5 (bending)	0	3.05	2.76
			Group 1
6 (bending)	1	5.73	
		5.75	
7 (bending)	2	5.83	
		5.84	
8 (bending)	3	5.96	
		5.98	
9 (torsion)	-	6.06	
10 (bending)	4	6.12	
11 (bending)	0	13.70	Group 2

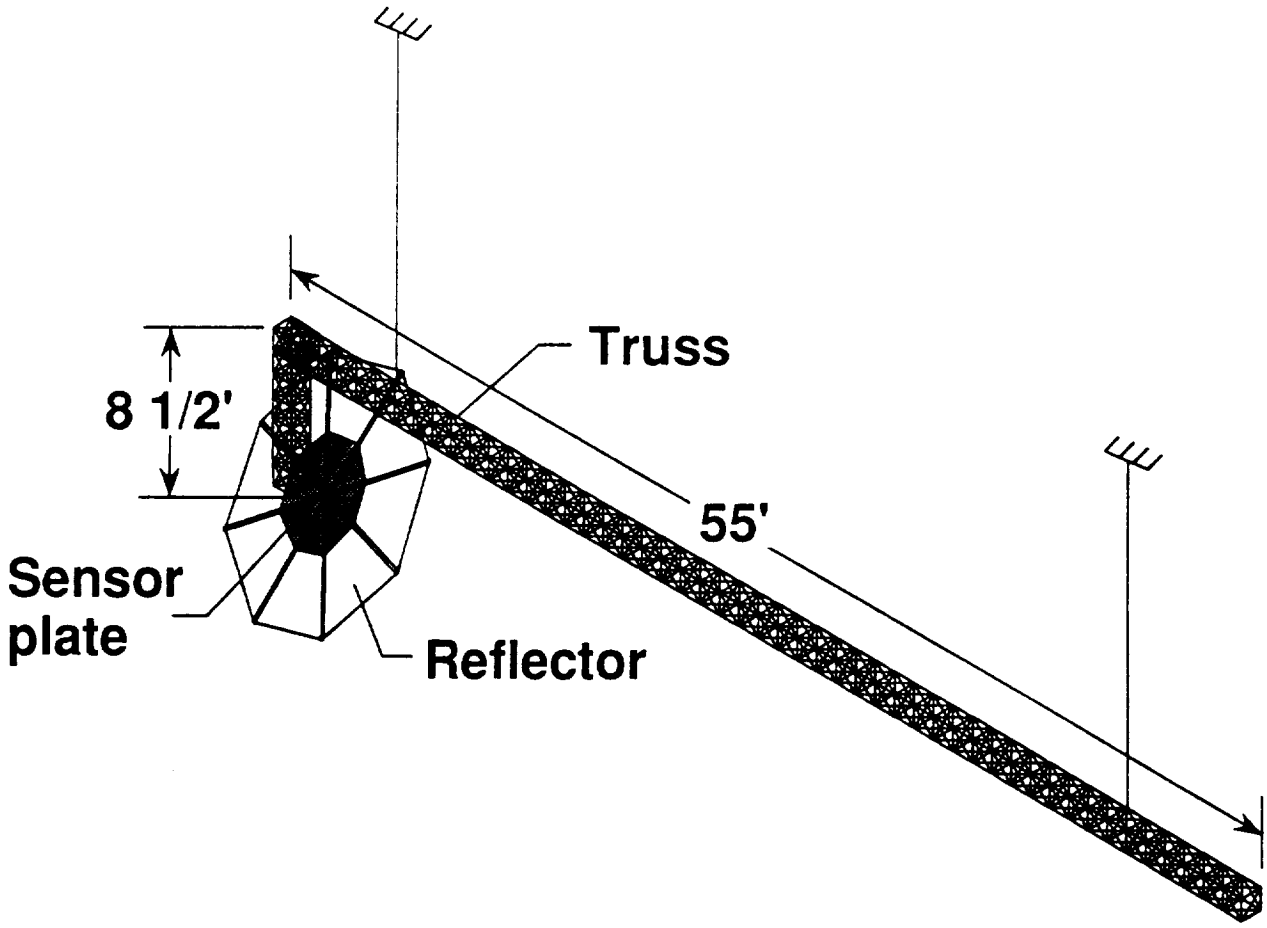

Fig. 1 CSI Evolutionary Model.

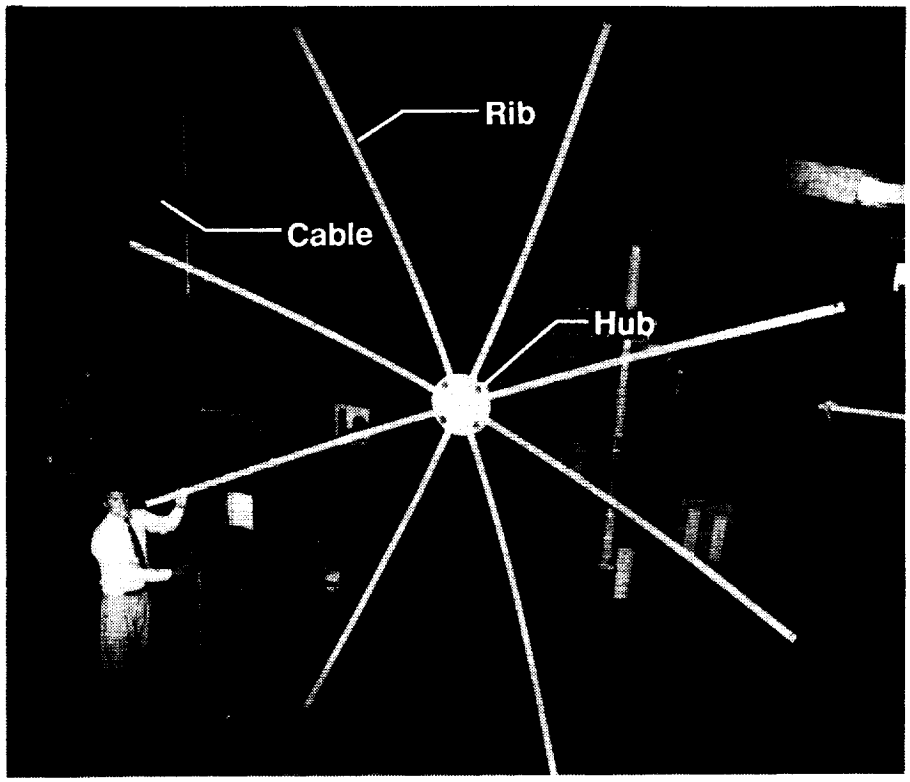

(a) Front view.

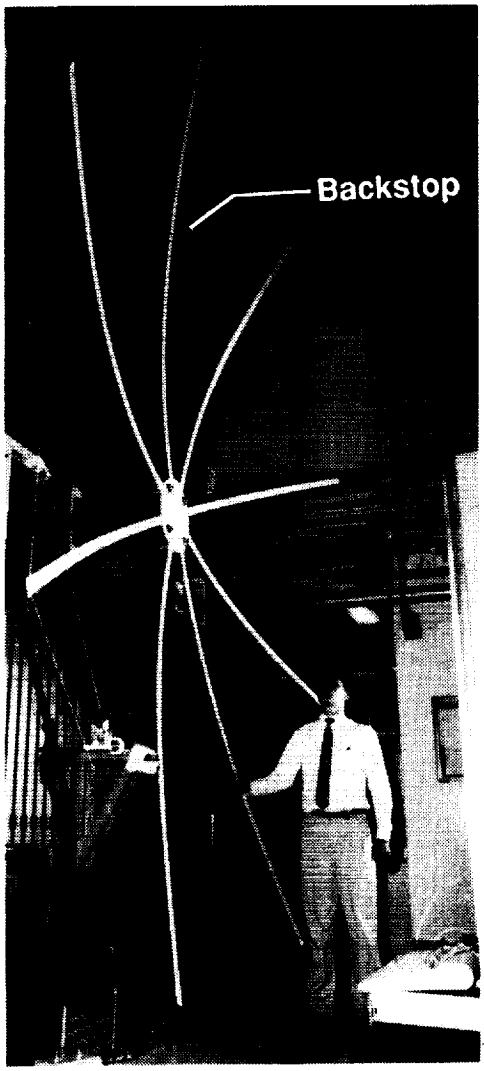

(b) Side view.

Fig. 2 Photographs of the 16-foot radial rib reflector model.

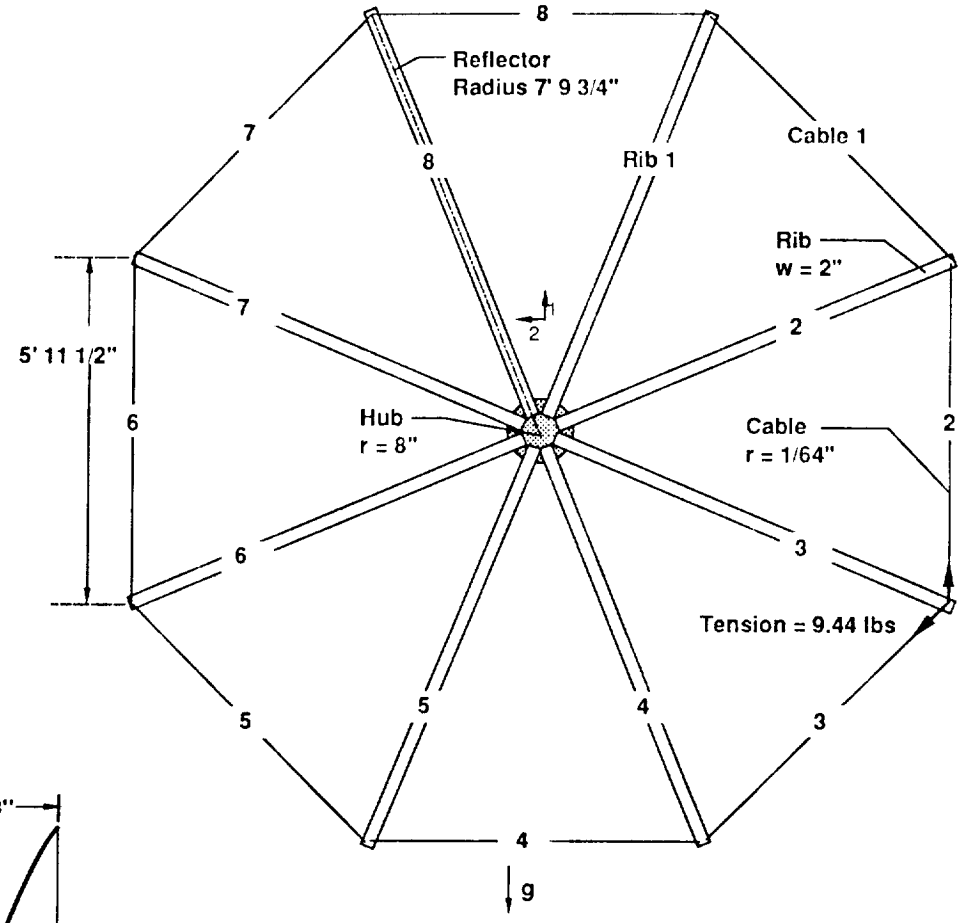

(a). Front view with rib and cable numbers for identification.

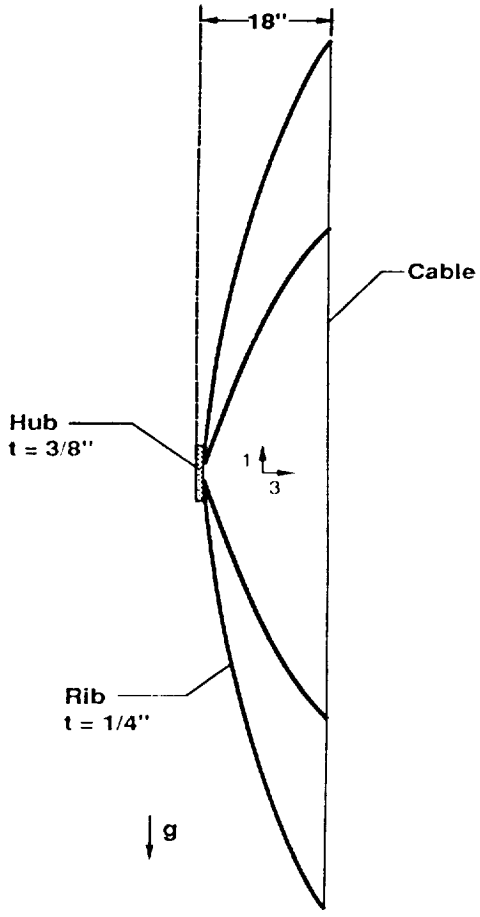

(b). Side view.

Fig. 3 Reflector test model with component dimensions.

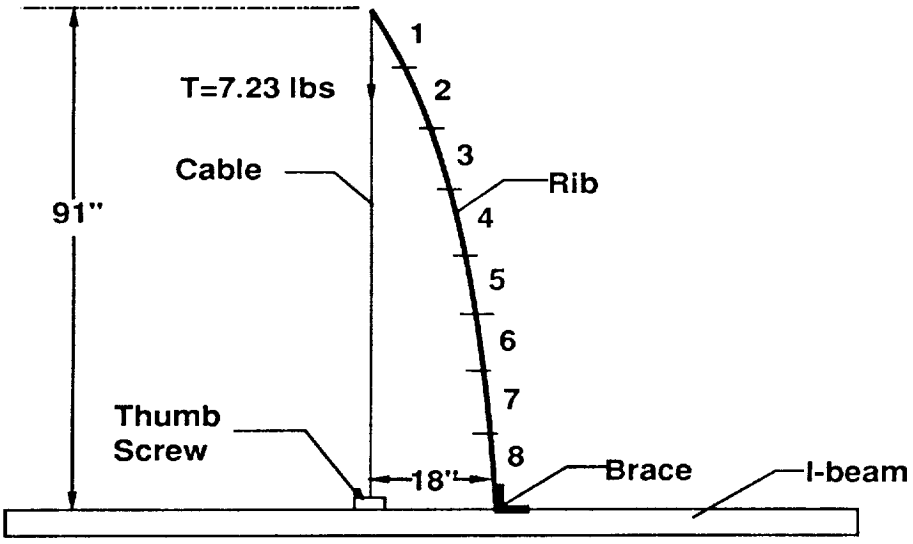

Fig. 4 Side view of single rib model with dimensions and element numbers.

Mode	Analytical Freq. (Hz.)	Experimental Freq. (Hz.)
1	2.88	2.9
2	13.56	13.05
3	21.28	21.3
4	34.71	36.55

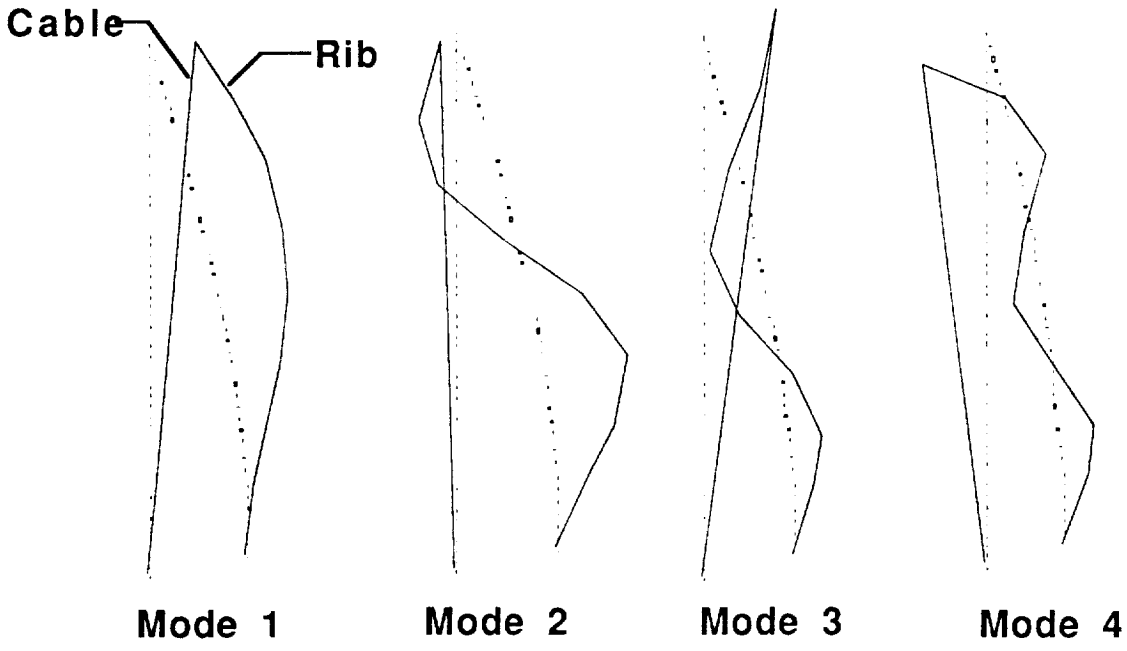

Fig. 5 Single rib frequency comparison with analytical mode shapes.

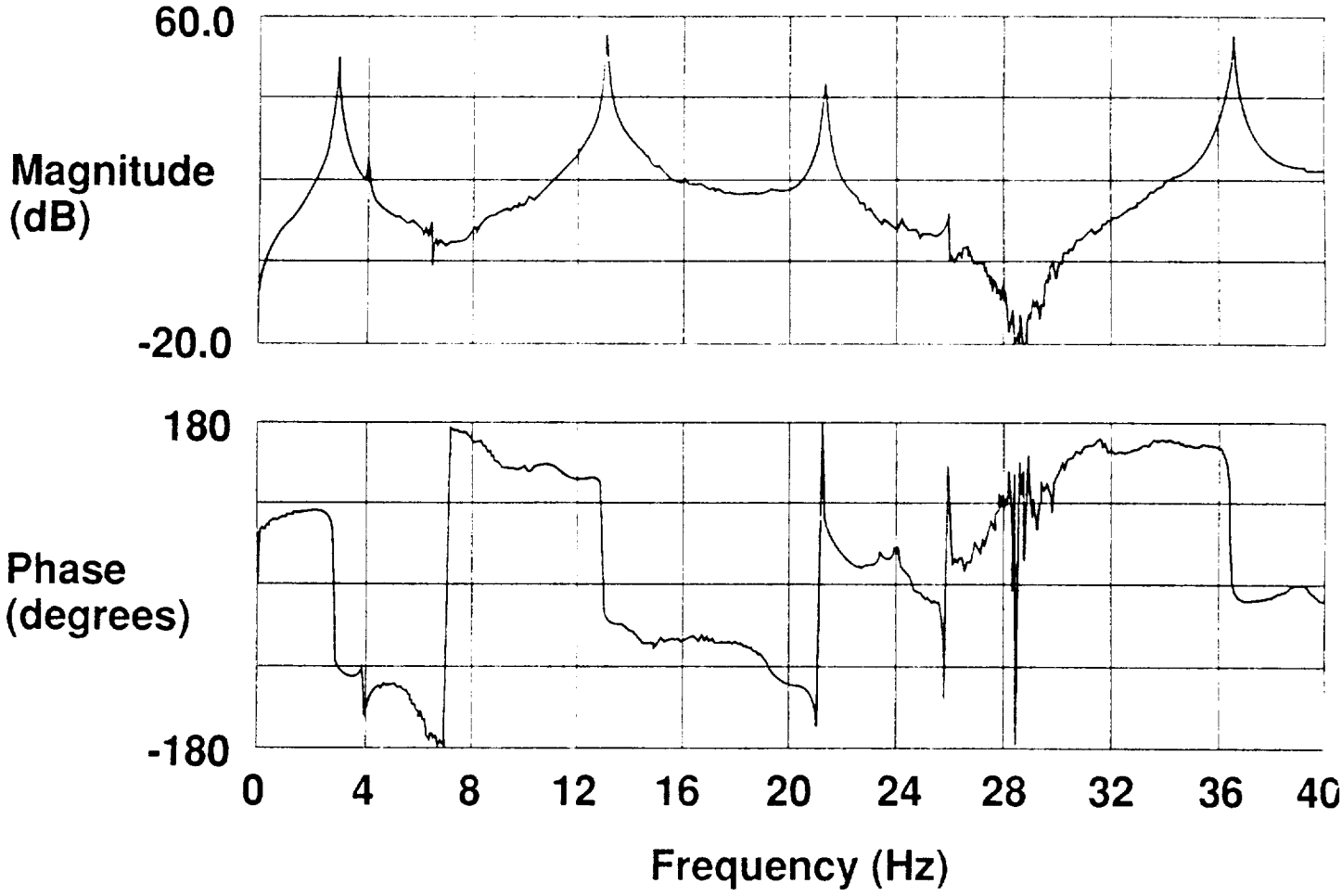

Fig. 6 Magnitude and phase plots of an averaged frequency response function from a single rib test.

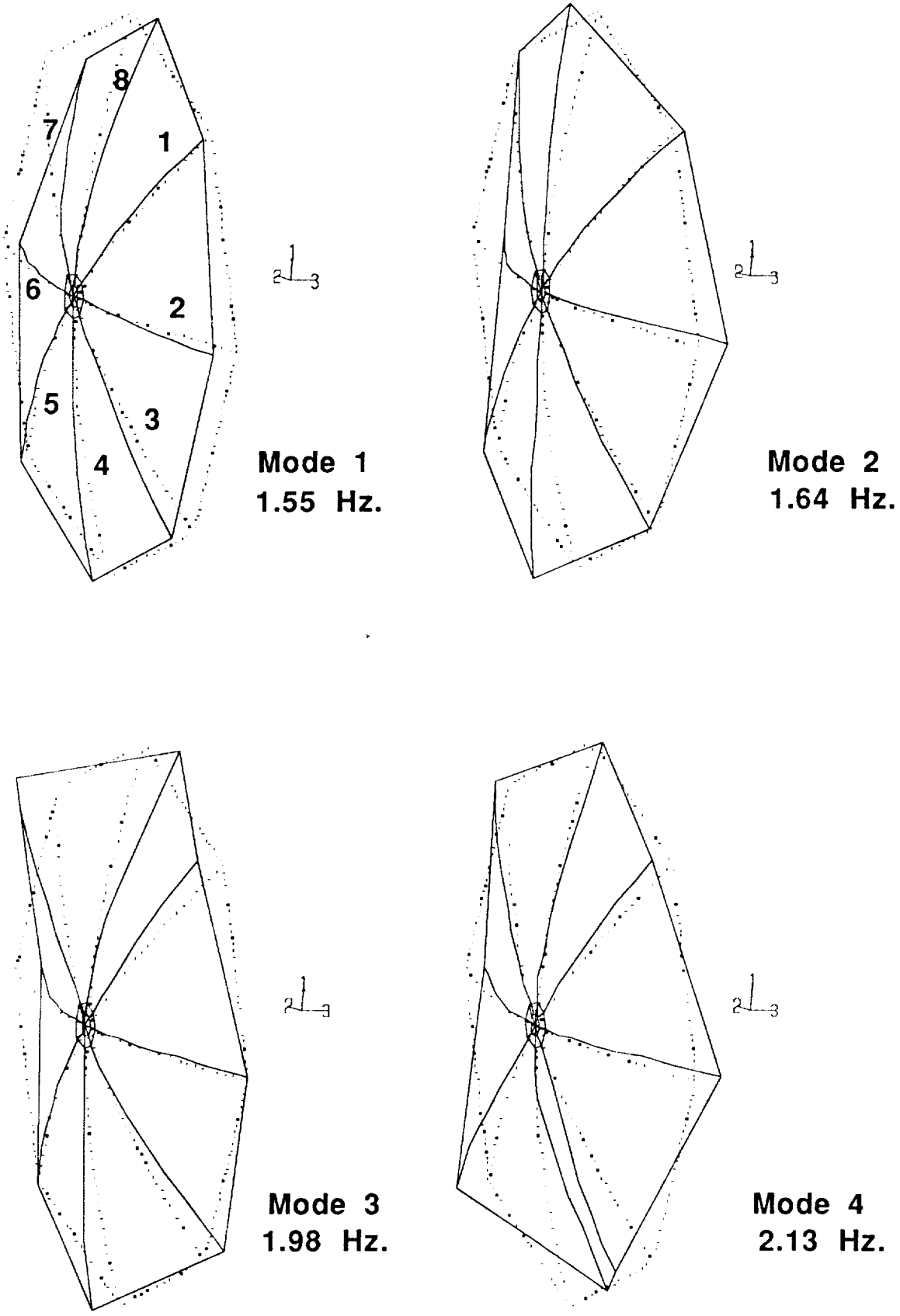

Fig. 7 Mode shapes and analytical frequencies of the reflector.

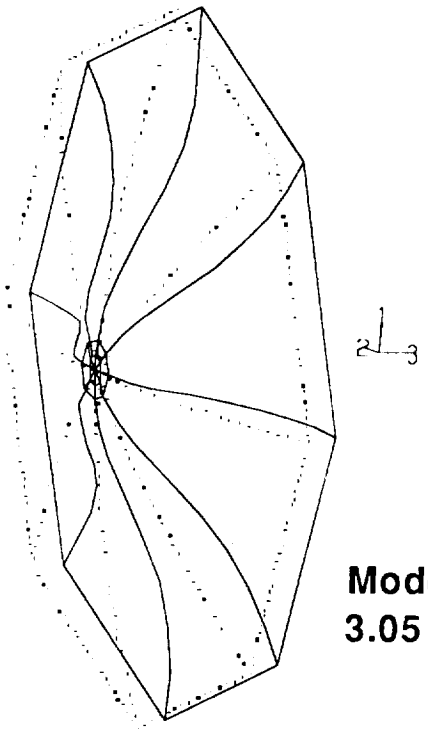

Mode 5
3.05 Hz.

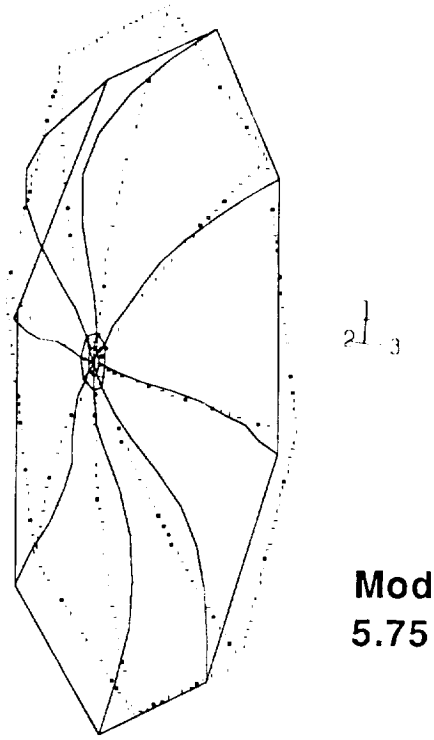

Mode 6
5.75 Hz.

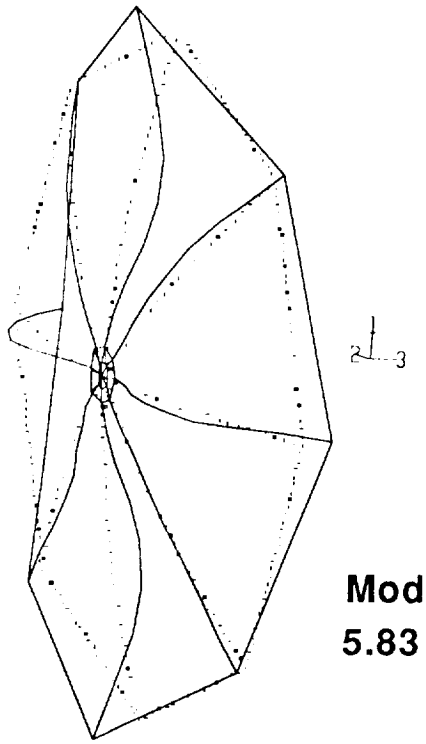

Mode 7
5.83 Hz.

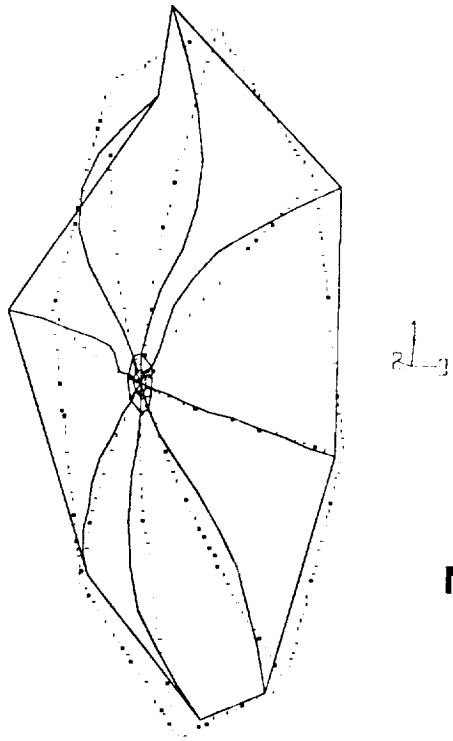

Mode 8
5.96 Hz.

Fig. 7 Continued.

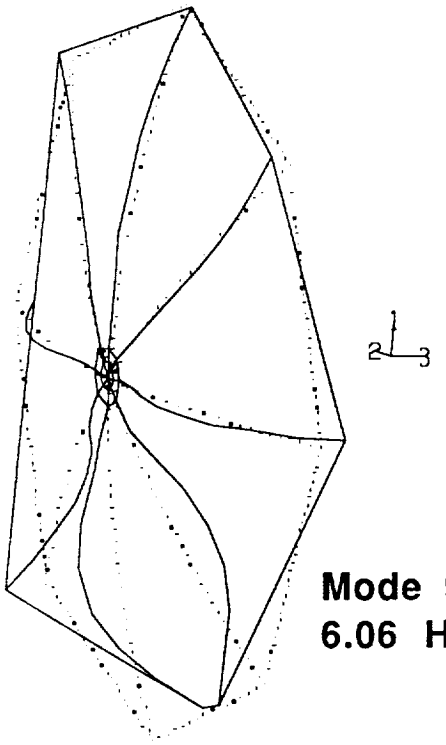

Mode 9
6.06 Hz.

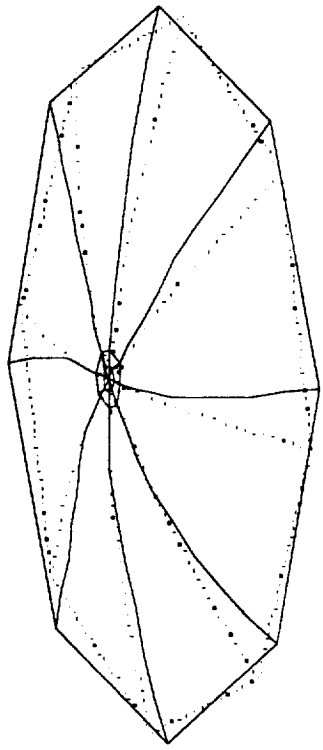

Mode 10
6.12 Hz.
Torsional

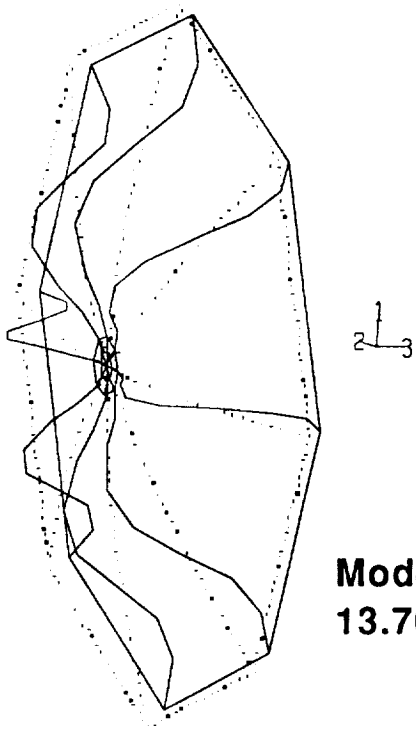

Mode 11
13.70 Hz.

Fig. 7 Continucd.

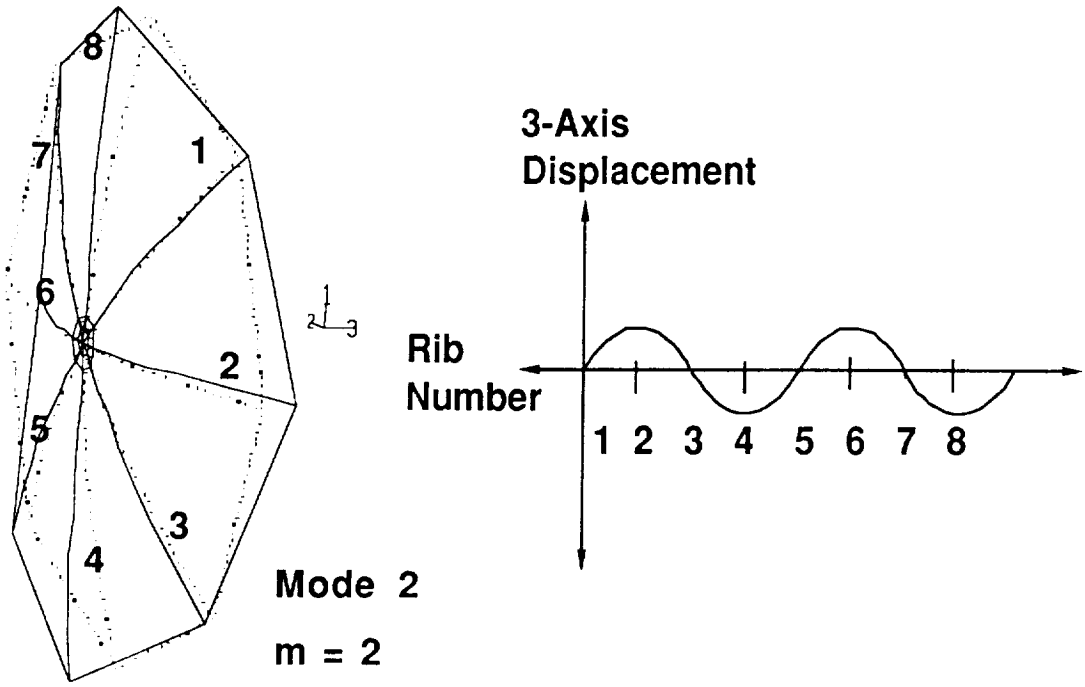

Fig. 8 Mode number determination method - rib number plotted vs. 3-axis displacement.

Appendix

This is a copy of the EAL run stream used to analytically model the 16-foot radial rib reflector model.

```
$ -- THIS EAL INPUT STREAM MODELS THE 16-FOOT RADIAL RIB
$ -- REFLECTOR DEVELOPMENTAL MODEL. CABLE DENSITY
$ -- AND LUMPED MASS MATRIX ARE CHANGES FROM THE ORIGINAL
$ -- RUNS. THE DEFORMED RIBS ARE IN THE ZERO LOAD SHAPE.
$ -- THE PRELOADS MUST BE ADDED AFTER THE GEOMETRY IS
$ -- INPUT. REFER TO THE COMMENTS TO UNDERSTAND THE INPUT
*CALL(18 PLB JCL)
*XQT U1
*(GEOM)                          END
*XQT TAB$
START 97
*ONLINE=1  $ -- USE EITHER ONLINE OR ECHO
S*ECHO=1
TITLE' ALUMINUM REFLECTOR WITH EIGHT RIBS, 16 FEET DIAMETER
TEXT
'1 RIB SIZE 2X1/4 INCHES
'2 FLN = FORTM1
MATC$
 1  10.E+06  0.333  0.098 2.0E-08        $ ALUMINUM RIBS AND PLATE
$ -- ALUMINUM COEFF. OF THERM EXPANSION SET FOR NUMERIC
$ -- CONVENIENCE WHEN APPLYING PRELOADS TO RIB ELEMENTS
 2  30.E+06  0.3    0.283             $STEEL BOLTS THROUGH PLATE AND RIBS
 3  30.0E+06   .3      0.177  -4.1047E-06 $  STEEL CABLE
S  THE COEFF. OF THERMAL EXPANSION FOR STEEL CABLE IS CALCULATED TO
S          INDUCE LOAD WHEN SUBJECTED TO 100 DEG. TEMP CHANGE
JLOC$
*FORMAT=2
$ -- GEOMETRY OF DEFORMED REFLECTOR
$ --  CENTER OF COOR. SYS IS AT PLATE CENTER, HALF-THICKNESS OF A RIB
1  93.7500  0.    18.1250   93.7500  315.0  18.1250   8  12
2  82.3125  0.    14.3750   82.3125  315.0  14.3750   8  12
3  70.8125  0.    11.0000   70.8125  315.0  11.0000   8  12
4  59.2500  0.     7.8125   59.2500  315.0   7.8125   8  12
5  47.6250  0.     5.1250   47.6250  315.0   5.1250   8  12
6  35.8750  0.     2.7500   35.8750  315.0   2.7500   8  12
7  23.9375  0.     1.0625   23.9375  315.0   1.0625   8  12
8  16.1250  0.     0.3125   16.1250  315.0   0.3125   8  12
9   7.7500  0.     0.0000    7.7500  315.0   0.0000   8  12
10  3.7500  0.     0.0000    3.7500  315.0   0.0000   8  12
11  7.7500  0.    -0.3125    7.7500  315.0  -0.3125   8  12
12  3.7500  0.    -0.3125    3.7500  315.0  -0.3125   8  12
97    0.0000   0.0000   -0.3750
```

```
$DESCRIBE THE COMPONENT GEOMETRY
BA$
 RECT 1  2.0  0.250  $  --  REFLECTOR RIBS, EXACTLY .25 X 2 IN.
 TUBE 2  0.0  0.125 $ 1/4 INCH BOLTS
BC
 1   .000767   $ --- 1/32 DIAMETER CABLE
SA
 NMAT=1
 FORMAT=ISOTROPIC
 1  .375  $  --  PLATE THICKNESS IS 3/8 IN.
MREF$
 1  2  3   1   0.
 2  1  2   1   1.0
CON=1  $  --  ORIGINAL CONSTRAINT CASE
ZERO 1 2 3 4 5    $ --- PLATE CLAMPED (CONSTRAINED)TO BACKSTOP
$  --  AT 4 BOLTS, EACH WITH 5 DOF'S
 24 :48 :72 :96    $   --- FOR ONE ROTATIONAL DOF
CON=2  $  --  ADDITIONAL CONSTRAINT CASE
 ZERO 1 2 3 4 5 6   $CONSTRAIN EVERYTHING TO APPLY LOADS IN K1 STIFF. MATRIX
  1,97,1
RMASS
 REPEAT 8,12
 11   .000371  $ POINT MASSES ADDED BECAUSE HUB IS MODELED AS
$        --  AN OCTAGON WHICH HAS SMALLER VOLUME THAN ACTUAL CIRCULAR PLATE
*XQT ELD
E23$
GROUP 1' OUTER RIM CABLES
  NMAT=3
  NSEC=1
 1 13  1  7  1  0
 85  1
E21$
GROUP 1' RADIAL RIBS
  NMAT=1   $ --- 2 X .25 INCH ALUMINUM STRIPS
  NSEC=1
  1  2  1  9  8  12
GROUP 2' BOLTS THROUGH HUB
NMAT=2
NREF=2
NSECT=2
  9  11  1  1  8  12
 10  12  1  1  8  12
E33$
GROUP 1' INNER TRIANGLES OF ANTENNA HUB
 NMAT=1
$ --- ALWAYS ALIGN ONE SIDE WITH COORDINATE AXIS
  97  12  24
  97  36  24
  97  36  48
  97  60  48
  97  60  72
  97  84  72
  97  84  96
```

```
  97  96  12
E43$
GROUP 1'OUTER QUADS OF ANTENNA HUB
 NMAT=1
$ ---  ALWAYS ALIGN ONE SIDE WITH COORDINATE AXIS
 12  11  23  24
 36  35  23  24
 36  35  47  48
 60  59  47  48
 60  59  71  72
 84  83  71  72
 84  83  95  96
 12  11  95  96
*XQT E$
 RESET G=386.0
*XQT EKS
*XQT TAN
*XQT K  $  --  ORIGINAL STIFFNESS MATRIX K-MATRIX CREATED
 RESET KFAC=0
*XQT RSI
 RESET CON=2
*XQT M
 RESET G=386.0
*END
*(TMAS)                          END
*XQT AUS
M1 = SUM(DEM,RMAS)   $ IF WANT CONSISTENT MASS MATRIX INSTEAD OF LUMPED
!MNAME=M1             $ MASS MATRIX, USE CEM, NOT DEM IN ABOVE LINE
*PERFORM(28 TMCG)
*RETURN
*END
*(SYSV)                          END
$  --  THIS IS THE INDEPENDENT SECTION WHICH IS RUN BY ITSELF TO
$  --   DETERMINE THE PRELOADS IN THE INDIVIDUAL RIB
$  --   ELEMENTS ONLY
*XQT AUS
ALPHA: CASE TITLE: 1' APPLY CABLE LOADS
SYSVEC: APPL FORC 1
 I=1:  J= 1:  -7.23      $ - VECTOR FORCE COMPONENTS OF CABLES APPLIED AT
$  --                  RIB TIPS
 I=1:  J=49:   7.23
 I=2:  J=25:  -7.23
 I=2:  J=73:   7.23
 I=1:  J=13:  -5.11
 I=2:  J=13:  -5.11
 I=1:  J=37:   5.11
 I=2:  J=37:  -5.11
 I=1:  J=61:   5.11
 I=2:  J=61:   5.11
 I=1:  J=85:  -5.11
 I=2:  J=85:   5.11
*XQT SSOL
*XQT VPRT
```

```
LINE=24
JOINT=1,12:49,60:13,24:61,72:25,36:73,84:37,48:85,96
TPRINT STAT DISP 1 1
*XQT ES
MAXPAGE=48
U = STAT DISP 1 1
E23
SE21 = PX,PY,PZ,MX,MY,MZ
E21
E33
E43
*XQT DCU
TOC 1
*END
*(ELDA)                          END   $ -PRELOAD APPLICATION SECTION
$                  COMPUTE PRELOAD
$                  ALPHA A = F/(DT * E * A)
*XQT AUS
ALPHA: CASE TITLE: 1' APPLY CABLE PRELOADS, 89/03/28
ELDATA:  TEMP E23 1
CASE 1
G=1: E=1,8: 100.0, 0., 0.    $  --  THERMAL CHANGES OVER CABLES
ELDATA:  TEMP E21 1
CASE 1
G=1:   E=1,64,9:   68.702,  0.0,  0.0
G=1:   E=2,65,9:   69.374,  0.0,  0.0
G=1:  E=3,66,9:  69.700, 0.0, 0.0  $  --  THERMAL CHANGES OVER RIB ELEMENTS
G=1:   E=4,67,9:   70.442,  0.0,  0.0
G=1:   E=5,68,9:   70.867,  0.0,  0.0
G=1:   E=6,69,9:   71.588,  0.0,  0.0
G=1:   E=7,70,9:   71.969,  0.0,  0.0
G=1:   E=8,71,9:   72.250,  0.0,  0.0
*XQT EQNF
*XQT SSOL
 RESET CON=2, SET=1 $ CONSTRAINT CASE 2 IS CALLED
$       -          ALL POINTS FULLY CONSTRAINED
*XQT GSF
 RESET EMBED=1, CON=2
*XQT PSF
 RESET DISPLAY=2
 E23: E21
*XQT KG
*XQT AUS
 K1=SUM(K,KG)  $ -- NEW STIFFNESS MATRIX CREATED: SUM OF ORIGINAL
$          K-MATRIX AND DIFFERENTIAL STIFFNESS OF PRELOADS ADDED
*END
*(GRAV)                          END
*XQT RSI
 RESET CON=1 K=K1
*XQT AUS
ALPHA: CASE TITLE: 1' APPLY GRAVTITATIONAL LOAD, 89/03/17
 RBM = RIGID (0.0, 0.0, 5.47)      $RIGID BODY MASS: APPLIED AT MASS CENTER
 DEFINE X1 = RBM AUS 1 1 1
```

```
 DEFINE X2 = RBM AUS 1 1 2
 VEC = SUM(.924 X1, .383 X2)  $ NEED TO ORIENT GRAV VECTOR CORRECTLY
 APPL FORC 2 = PROD(-386.1 M1, VEC)
*XQT EQNF
 RESET SET=2
*XQT SSOL
 RESET K=K1
 RESET CON=1, SET=2
*XQT GSF
 RESET EMBED=1, CON=1, SET=2
*XQT KG  $  --  GRAV. DIFFERNTIAL STIFFNESS MATRIX FORMATION
*XQT AUS
 KTOT=SUM(KG,K1) $ ADDING GRAV DIFFERENTIAL STIFF. MATRIX, KG,
$  TO NEW STIFFNESS MATRIX K1 TO COME UP WITH FINAL K-MATRIX, KTOT
*XQT VPRT
 PRINT EQNF
 PRINT STAT DISP  $  THESE LINES PRINT OUT REATIONS AND DISPLACEMENTS
 PRINT STAT REAC
*END
*(VIBR)                          END   $EIGENVALUE SOLUTION
*XQT E4
 RESET M=M1 K=KTOT CON=1
 RESET NMODES = 17
*XQT DCU
 TOC 1
*XQT VPRT
 TPRINT VIBR MODE      $ TO GET THE EIGENVECTORS
* END
*(PLTU)                           END   $  PLOTTING COMMANDS
*ECHO=1
*FREE 18
*XQT PLTA
SPEC 1
STITLE'4 PTS. ON PLATE ARE TOTALLY CONSTRAINED
S2TITL'16 FOOT DIAM REFLECTOR, W/GRAVITY
VIEW 3
ROTATE 67,3   60,1   23,2
AXES 0., 0., 90., 10., 10., 10.
ALL
SPEC 2
STITLE'4 PTS. ON PLATE ARE TOTALLY CONSTRAINED
S2TITL' 16 FT DIAM REFL, BARS 2X1/4
VIEW  1,-3,2,1
LROTATE 67,3   180,1
AXES -75., 80., -25., 20., 20., 20.
ALL
*XQT PLTB
DISPLAY=VIBR
INLIB=1
CASES 1,17   $MAKE SURE THIS IS SET TO THE APPROPRIATE NUMBER OF CASES
DNORM=15.0
OPTION  26,27
PLOT  1  ,2
```

```
*END
*DCALL(GEOM)        $ GEOMETRY CARD CALLED
*DCALL(TMAS)        $ MASS MATRIX FORMED
$*DCALL(SYSV)  $ THIS-SECTION IS USED BY ITSELF, ONLY TO SOLVE FOR
$                  INDIVIDUAL RIB ELEMENTAL LOADS
*DCALL(ELDA)     $ PRELOADS APPLIED WITH THERMAL CHANGES (FULL CONSTRAINT)
*DCALL(GRAV)   $ GRAV. LOAD APPLIED (CORRECT CONSTRAINT CASE)
*DCALL(VIBR)  $ VIBRATIONAL ANALYSIS TO GET EIGENVALUES AND EIGENVECTORS
*DCALL(PLTU)  $ PLOT CARD
*XQT EXIT
```

NASA National Aeronautics and Space Administration

Report Documentation Page

1. Report No.	2. Government Accession No.	3. Recipient's Catalog No.
NASA TM-101648		

4. Title and Subtitle	5. Report Date
Analysis and Test of a 16-Foot Radial Rib Reflector Developmental Model	August 1989
	6. Performing Organization Code
7. Author(s)	8. Performing Organization Report No.
Shawn A. Birchenough	
	10. Work Unit No. 585-01-61-01
9. Performing Organization Name and Address	11. Contract or Grant No.
NASA Langley Research Center Hampton, VA 23665-5225	
	13. Type of Report and Period Covered
12. Sponsoring Agency Name and Address	Technical Memorandum
National Aeronautics and Space Administration Washington, DC 20546-0001	14. Sponsoring Agency Code

15. Supplementary Notes

Shawn A. Birchenough is a student at the Massachusetts Institute of Technology. This work was accomplished during an engineering cooperative education work assignment at the Langley Research Center.

16. Abstract

Analytical and experimental modal tests have been performed to determine the vibrational characteristics of a 16-foot diameter radial rib reflector model. Single rib analyses and experimental tests provided preliminary information relating to the reflector. A finite element model predicted mode shapes and frequencies of the reflector. The analyses correlated well with the experimental tests, verifying the modeling method used. The results indicate that five related, characteristic mode shapes form a group. The frequencies of the modes are determined by the relative phase of the radial ribs.

17. Key Words (Suggested by Author(s))	18. Distribution Statement
Antennae model Radial rib Finite element analysis Ground vibration tests	Unclassified - Unlimited Subject Category 39

19. Security Classif. (of this report)	20. Security Classif. (of this page)	21. No. of pages	22. Price
Unclassified	Unclassified	26	A03

NASA FORM 1626 OCT 86